

# Path-Constrained State Estimation for Rail Vehicles

Cornelius von Einem<sup>1,\*</sup>, Andrei Cramariuc<sup>2,\*</sup>, Roland Siegwart<sup>1</sup>, Cesar Cadena<sup>1</sup> and Florian Tschopp<sup>3</sup>

**Abstract**—Globally rising demand for transportation by rail is pushing existing infrastructure to its capacity limits, necessitating the development of accurate, robust, and high-frequency positioning systems to ensure safe and efficient train operation. As individual sensor modalities cannot satisfy the strict requirements of robustness and safety, a combination thereof is required. We propose a path-constrained sensor fusion framework to integrate various modalities while leveraging the unique characteristics of the railway network. To reflect the constrained motion of rail vehicles along their tracks, the state is modeled in 1D along the track geometry. We further leverage the limited action space of a train by employing a novel multi-hypothesis tracking to account for multiple possible trajectories a vehicle can take through the railway network. We demonstrate the reliability and accuracy of our fusion framework on multiple tram datasets recorded in the city of Zurich, utilizing Visual-Inertial Odometry for local motion estimation and a standard GNSS for global localization. We evaluate our results using ground truth localizations recorded with a RTK-GNSS, and compare our method to standard baselines. A Root Mean Square Error of 4.78 m and a track selectivity score of up to 94.9% have been achieved.

## I. INTRODUCTION

Railway passenger numbers are steadily increasing with increasing environmental awareness and widespread demand for more personal mobility. Simultaneously, governments are pushing to increase global trade volumes via rail transport rather than truck and air freight. These factors push the current railway networks closer to their maximum operational capacity. New modes of operation and technologies are needed to facilitate more trains without building new tracks. Most railway network safety systems, such as the European Train Control System (ETCS) Level 0-2 [1], operate using fixed block interlocking. In ETCS, motion authority is granted to incoming vehicles only if entire track segments are guaranteed to be free using sparse track-side infrastructure beacons (Balises). A more efficient moving block strategy would permit for a denser operation of the network but would require accurate and continuous knowledge of the position of each train [2]–[4]. To ensure the safe operation of the network, we need to know the specific track the vehicle is located on and where along the track it is. This is to guarantee

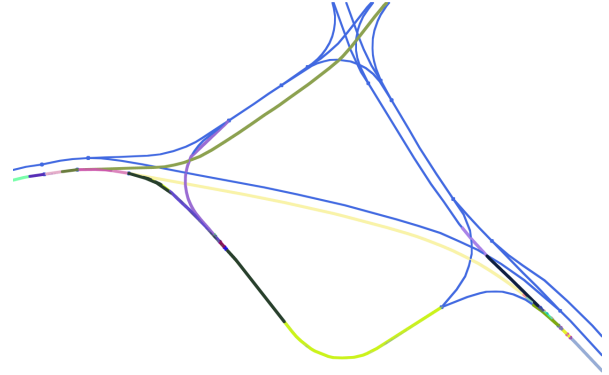


Fig. 1: Multiple filter hypotheses following each track (blue) through the rail network. Each color represent one motion trajectory hypothesis.

sufficient braking distances, as well as to detect wrong turns or either missed or faulty signals at switches.

For railways, a lot of focus has been on the use of Global Navigation Satellite System (GNSS) [2], [5] for global positioning. However, GNSS has many modes of failure, and for higher levels of reliability, multiple independent modalities need to be combined [6]. Typical sensor fusion systems employ some variant of filtering, such as a particle filter or a Kalman Filter (KF), to integrate various modalities into a common state space representation. However, using standard approaches that represent the state as a 3 Degrees of Freedom (DoF) or 6 DoF leads to estimates that are in reality impossible, *i.e.* a train can not be outside the tracks. These approaches also do not accurately reflect the uncertainty of which track the vehicle is most likely on, just that it is somewhere off-track. Many commonly used sensors, including GNSS, also do not provide measurements that are constrained to the tracks. Currently, existing sensor fusion approaches for rail networks are map-agnostic and do not leverage this extremely useful information [7], [8].

In this work, we specifically address railway networks and propose a novel state estimation framework, tailored to the constraints of the environment. We design our own Extended Kalman Filter (EKF) to track the position of a singular vehicle over time. Since rail vehicles can only move in a line, we model the state space of the filter as the distance traveled along a specific track, where we define a track as the rail segment between two intersections. In combination with known and publicly available track maps, a full 6DoF pose of the vehicle can always be recovered. We propose a novel way to transfer sensor measurements from different

\*Authors contributed equally to this work

<sup>1</sup>Authors are members of the Autonomous Systems Lab, ETH Zurich, Switzerland; {firstname.lastname}@mavt.ethz.ch

<sup>2</sup>Author is a member of the Robotics Systems Lab, ETH Zurich, Switzerland but the work was done while the author was a member of <sup>1</sup>; {firstname.lastname}@mavt.ethz.ch

<sup>3</sup>Author is with Arrival Ltd., London, United Kingdom; tschopp@arrival.com

This work was supported by the ETH Mobility Initiative under the project LROD-ADAS.

modalities into this 1D track space to update the filter state. In doing this projection, we also gain additional insight into the correctness of our estimate from the map information. We implicitly check that the geometry of the estimated motion matches the shape of the track, *e.g.* if the motion estimate goes in a line but on the map we have a curve, the uncertainty of our estimate should increase.

Ordinary EKF's can only track a singular state hypothesis, which does not reflect well the various possible trajectories a vehicle can take through the network. *E.g.*, we do not want an error at an intersection to cause the train to be localized on the adjacent track. We represent this by utilizing a collection of EKF's that track multiple possible movement hypotheses, sampling new filters at intersections and removing ones that have diverged due to disagreeing sensor updates, as shown in Figure 1. To evaluate the agreement between individual sensor measurements and each state hypothesis, we integrate a cost function and outlier rejection scheme into the EKF's. We evaluate our framework extensively on real-world data from trams in the city of Zürich, using a GNSS for global positioning and a Visual-Inertial Odometry (VIO) algorithm for motion estimation. However, our method remains generic and can be applied to other global and motion estimation sources, such as wheel odometers, Inertial Measurement Units (IMUs) or Balises. To summarize, our contributions are as follows:

- A path-constrained EKF formulation and update scheme for modeling the movement of rail vehicles along a known rail network.
- An EKF-based multi-hypothesis tracking scheme for observing various possible vehicle trajectories throughout the railway network.
- Extensive evaluations on a real-world dataset, recorded on trams in Zurich, Switzerland. We do not only focus on correct track identification but also evaluate the accuracy of the position along the track.

## II. RELATED WORK

### A. Sensor Fusion

Sensor fusion is necessary to compensate for failure modes of different modalities and has seen two main-stream approaches. First, filter-based approaches, such as particle filters [9], [10] and Kalman Filters (KFs) [11]–[13] with many variants and extensions. Second, sliding window-based optimization approaches [14], [15] that create a local factor graph and use a non-linear optimizer to solve the unknown states. Except for particle filters, none of the other approaches is implicitly able to handle multiple hypotheses, which has shown to be beneficial, for example in tracking [16] or landmark association [17]. To the best of our knowledge, our approach is the first to propose using a collection of Extended Kalman Filters (EKF's) to track and rank multiple hypotheses simultaneously. The only similar approach is the multi-hypothesis EKF proposed by Tan *et al.* [18] that uses only a single filter with multiple internal hypotheses for soft shape estimation.

### B. Map-aided Localization

Cars and trucks are limited to roads [19], [20], trains are limited to their tracks [3], and even ships are partially limited to rivers or stick to shipping lanes in the open oceans [21]. Knowledge of these paths (*i.e.* maps) can aid the localization process to achieve more accurate and reliable results, especially when paths present unique geometries [22]. A common approach is so-called map-matching, where the current vehicle state (*i.e.* pose) or its recent trajectory is matched to certain state possibilities on a map. Quddus *et al.* [23] analyzed various map-matching algorithms and their limitations. Point-to-point matching [24] is highly sensitive to the resolution of the map, leading to easy failure cases. Point-to-curve [25]–[28] or curve-to-curve matching [29], [30] methods allow for more robust state estimation independent of sensor modalities by comparing local estimates to curves in the map. To improve the robustness of these matching schemes, one can incrementally match larger segments [31], introduce voting schemes [32], or candidate graphs [33]. However, these approaches all model the vehicle state as being feasible in the entire Euclidean space and use map data only to post-correct the position estimates, which can lead to poor track selectivity, *i.e.* unreliable knowledge of which track the vehicle is located on.

In contrast, the vehicle position can be constrained from the beginning always to be located on a path. This is achievable using a histogram filter [34], though the downside is the discretization of the state space. Other options include particle filters [35], [36] with the drawback of complicated path-constrained particle re-sampling. Operating in curve coordinates along the pre-defined paths results in a natural description of the vehicle kinematics and allows for the usage of KFs [30], [37], [38]. An inherent issue of these KFs is the branching of paths, where wrong choices in the intersection lead to unrecoverable failures in the state estimation. Our proposed approach re-designs the KF-based approach to seamlessly combine path-constrained state estimation with multi-hypothesis tracking into one unified framework aimed at rail networks.

### C. State Estimation for Trains

Switching existing railway networks from a low-resolution infrastructure side localization system, using track-mounted Balises, to an accurate and continuous state estimation would enable train operators to deploy significantly more trains on the existing tracks while ensuring current levels of safety [39]. GNSS is an obvious choice for the global localization of trains [2], [5]. However, GNSS is highly dependent on a clear view of the sky and can easily be obstructed through jamming devices [6], so it is not suitable for safety-critical applications and should be fused with other modalities. Different other methods have been proposed for positioning rail vehicles, from RFID tags [40], [41], magnetic sensors [42], [43], vibration signatures [44], vision [45], to LiDARs [46], [47]. Similarly, drifting local motion estimation can be done using a variety of modalities, such as IMUs and wheel odometers [48], Doppler radars [8], or vision [49],



where  $s$  and  $\dot{s}$  are the traveled distance and velocity along that track, respectively. As the track itself is also an important part of the vehicle's state, it needs to be included as well, which is described in Section III-D and omitted here for simplicity.

1) *Filter propagation*: The standard state transition and observation models of an EKF are:

$$\begin{aligned} \mathbf{x}_k &= f(\mathbf{x}_{k-1}, \mathbf{u}_k) + \mathbf{Q}_k \\ \mathbf{z}_k &= h(\mathbf{x}_k) + \mathbf{R}_k, \end{aligned} \quad (4)$$

where  $\mathbf{x}_k$  represents the current state,  $\mathbf{u}_k$  the control input,  $\mathbf{z}_k$  the measurement,  $\mathbf{Q}_k$  the process noise, and  $\mathbf{R}_k$  the measurement noise. The general motion of the rail vehicle in 6DoF is non-linear due to the forces applied by the train tracks onto the train, restricting its freedom of motion. The linearization of this process model happens indirectly through the choice of curve-coordinates and allows for a simple formulation of the state transition in 1D coordinates. As we do not consider a control input at the moment, this simplifies the process model to:

$$\begin{aligned} \mathbf{x}_{k|k-1} &= \mathbf{F} \hat{\mathbf{x}}_{k-1|k-1} \\ \mathbf{P}_{k|k-1} &= \mathbf{F}_k \mathbf{P}_{k-1|k-1} \mathbf{F}_k^T + \mathbf{Q}_k \\ \mathbf{F} &= \begin{bmatrix} 1 & \delta t \\ 0 & 1 \end{bmatrix}, \end{aligned} \quad (5)$$

where  $\mathbf{F}$  is the transition model,  $\mathbf{P}$  the state covariance and  $\mathbf{Q}$  the process noise.

2) *Measurement update*: Due to the special state space formulation, measurement updates will be non-linear as they are typically reported in Euclidean coordinates and need to be transformed into curve-coordinates. GNSS position updates, for example, will most likely lie somewhere in the vicinity of the tracks, but never precisely on a 1D track. This update can be integrated as the conditional probability distribution of the measurement given that the state has to be located on the tracks. Assuming a straight track and a symmetric Gaussian distribution, this conditional distribution is another normal distribution centered around the mean point projected onto the track, with the same standard deviation. When projecting a measurement onto a track, its coordinate system can, therefore, be changed from Euclidean to curve-coordinates.

The second key part of our measurement update step is an outlier rejection scheme to remove noisy measurements. This is implemented in the form of a measurement acceptance gate [52]. The projection of a measurement from Euclidean space to curve coordinates, similar to the projection of one vector onto another, also results in an error term  $\epsilon$ , that is perpendicular to the tracks. Based on the relation of this measurement term and the innovation covariance  $\mathbf{S}$ , a measurement is either accepted or rejected, and the state covariance is accordingly either updated or punished. If the error term  $\epsilon$  is smaller than  $\kappa\sqrt{\mathbf{S}}$ , where  $\kappa$  is a tuning parameter, the measurement is accepted. If the measurement is rejected, no measurement update is performed, and instead a punishment is applied to the state covariance. This

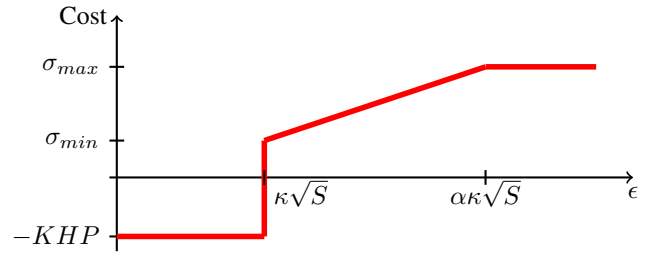


Fig. 4: Measurement acceptance gate cost function for outlier rejection.

punishment increases linearly from  $\sigma_{min}$  to  $\sigma_{max}$  until a second threshold of  $\alpha\kappa\sqrt{\mathbf{S}}$  is reached, after which only the maximum punishment is added to the state covariance. This can be expressed mathematically as shown in Equation 7 and is visualized in Figure 4.

The resulting measurement update equations are thus:

$$\begin{aligned} \mathbf{y}_k &= \rho(\mathbf{z}_k) - \mathbf{x}_{k|k-1} \\ \mathbf{S}_k &= \mathbf{H}_k \mathbf{P}_{k|k-1} \mathbf{H}_k^T + \mathbf{R}_k \\ \mathbf{K}_k &= \mathbf{P}_{k|k-1} \mathbf{H}_k^T \mathbf{S}_k^{-1} \\ \mathbf{x}_{k|k} &= \mathbf{x}_{k|k-1} + \mathbf{K}_k \mathbf{y}_k \\ \mathbf{m} &= \frac{\sigma_{max} - \sigma_{min}}{(\alpha - 1)\kappa\sqrt{\mathbf{S}}} \\ \mathbf{P}_{k|k} &= \begin{cases} (\mathbf{I} - \mathbf{K}_k \mathbf{H}_k) \mathbf{P}_{k|k-1} & \epsilon \leq \kappa\sqrt{\mathbf{S}} \\ \mathbf{P}_{k|k-1} + \mathbf{m}(\epsilon - \kappa\sqrt{\mathbf{S}}) + \sigma_{min} & \text{else} \\ \mathbf{P}_{k|k-1} + \sigma_{max} & \epsilon > \alpha\kappa\sqrt{\mathbf{S}} \end{cases} \end{aligned} \quad (6)$$

$$(7)$$

where  $\mathbf{H}$  is the observation model, selecting the parts of the state space which are observable by a specific sensor. For an odometry update, this is  $\mathbf{H} = [0 \ 1]$  and for GNSS the reverse.

Using this, GNSS updates can be integrated easily. The projection function  $\rho(\cdot)$  finds the closest point to the current track, which is then used for the sensor update. This distance to the track is the error term  $\epsilon$ .

The integration of odometry requires a few extra steps, since we utilize drifting VIO. The projection function  $\rho(\cdot)$  computes the velocity component parallel to the track, at the current position estimate, while the perpendicular component represents  $\epsilon$ , and is used for the outlier rejection step. As the motion estimate will drift over time, it will be increasingly misaligned from the true motion of the vehicle, leading ultimately to a failure of the EKF. However, based on the current track geometry around the current position estimate, we can realign the odometry to correct this drift. This is done in periodic intervals of 100m to reduce the impact of drift, but not in close vicinity to switches, as there are multiple possible position hypothesis with severely different vehicle orientations. This will be elaborated in further detail in Section III-D.2.

#### D. Multi-Hypothesis tracking

The previously described path-constrained EKF is capable of estimating the vehicle’s state along a singular track. For a real railway network, this is not sufficient as there are often multiple parallel tracks, switches, and crossings. There, even small amounts of sensor noise can lead to ambiguity, especially between parallel tracks. Thus, we propose to use a collection of EKFs to keep track of multiple possible hypotheses throughout the rail network.

1) *Initialization*: The first step is the initialization of the filters. After receiving a first global localization measurement (e.g., from GNSS), EKFs are spawned on all tracks within a radius of 100 m.

2) *Transition*: At each time step, all filters propagate according to their process model described in equation 5. If a measurement update is available, it is applied to all filters. Still, due to the outlier rejection and local track geometry, the resulting updates are different for each filter, leading to all filters propagating independently with differing covariances. Suppose a filter is near a map point that connects the current track to another one. In that case, an additional filter is created on the new track with equal velocities and covariance to maintain continuity in the transition. An exemplification of this can be seen in Figure 1. The VIO plays a significant role at these switches, as it will be more in accordance with one of the hypotheses over the other, which is why no odometry re-alignment occurs close to a switch.

3) *Filter removal*: Filters can be removed from the collection of active filters under several circumstances:

- A filter reaches the end of its associated track. As this is also the end of the respective coordinate space, the filter cannot continue and gets deleted.
- Measurements will not agree with the hypotheses maintained by some of the filters and will cause these filters to diverge. As the covariance of a filter increases above a certain threshold, the filter is retired and removed from the active collection.
- The third option for removing filters is pruning. Railway tracks naturally split and merge throughout the network. This can lead to multiple hypotheses being located on the same track and close to each other. To prevent these filters from converging to one state, the filter with lower covariance is removed when two filters approach one another.

4) *Maximum Likelihood Estimate (MLE) selection*: At each time step, a MLE is selected. This corresponds to the filter with the lowest positioning covariance at each time step. In addition, a low-pass filter is applied to this selection step, meaning that a certain filter needs to have the highest covariance for multiple time steps, to become the MLE. The track ID and position along that track for the current MLE is reported as the current state estimate of the entire system.

## IV. EXPERIMENTAL EVALUATION

To evaluate the accuracy and reliability of our path-constrained state estimation system, we performed multiple

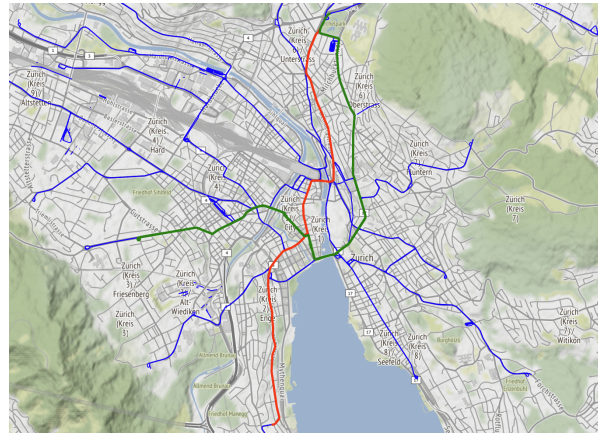


Fig. 5: Map of the city of Zurich. Tram tracks are highlighted in blue, Tram 7 (Trajectory 1) in red and Tram 9 (Trajectory 2 and Trajectory 3) in green.

experiments on real-world railway datasets. Furthermore, we directly compare the performance of our path-constrained estimator to a standard unconstrained EKF. Although a comparison to several of the other named railway state estimation frameworks would be informative, there are often specific to the utilized sensors which were not available to us.

#### A. Datasets

The framework was evaluated on three available datasets from trams in Zurich, Switzerland. Trajectory 1 was recorded on Tram line 7, has a length of 6812m and a duration of 26 min. Trajectory 2 was recorded on Tram line 9, has a length of 5980m and a duration of 23 min. Trajectory 3 was also recorded on Tram line 9 but is significantly longer with a length of 9544 m and a duration of 45 min. All three trajectories feature a variety of different environments, ranging from the dense city center with limited GNSS availability to outside residential areas with a clearer view of the sky. With many intersections and high buildings obstructing the GNSS signal, this environment is more challenging than most common railway environments. OpenStreetMap data was used as a ground truth track map and was filtered to only contain tracks belonging to the tram network of the city of Zurich, see Figure 5.

#### B. Hardware Setup

1) *Devices*: Localization data for the purpose of state estimation was obtained using a uBlox EVK-F9P GNSS evaluation kit, capable of receiving the  $L_1$  and  $L_2$  bands of the GPS, Galileo, BeiDou, and GLONASS satellite constellations. For Trajectory 1, the receiver was mounted outside the tram for a clear view of the sky. For Trajectory 2 and 3, the receiver was attached on the inside of the tram behind the glass of the window, resulting in a reduced GNSS signal. Vehicle odometry was recorded using a Skybotix VI-Sensor [53], consisting of two grayscale cameras at a resolution of  $752 \times 480$ px and at a frame

rate of 25 hz, as well as an ADIS16488 IMU recording at a rate of 200 hz. The device was mounted to record out of a side window of the tram. The odometry itself was computed using OKVIS [14] without any post-processing and thus significantly drifts over time. Ground truth positioning data was obtained using a PIKSI Multi Real-Time Kinematic (RTK)-GNSS, whose antenna was mounted on the outside of the tram for optimal positioning accuracy. As a post-processing step, the ground truth positioning data was projected on the ground truth track in the map, which is known from the public transportation map. Even though the state estimation system is significantly more complex than comparable baselines, it runs in real-time on a single core of an Intel Core i7-10875H CPU, not including the VIO as this is not a direct part of the framework,

2) *Calibration*: The intrinsic camera parameters of the VI-Sensor have been calibrated using the *Kalibr* toolbox [54] and a standard calibration board. At the time of recording, no appropriate calibration procedures were available for calibrating the VI-sensor and the various GNSS antennas relative to the train. Relative orientations were therefore obtained through manual tuning, while relative translations have been neglected and were accepted as a minimal source of error in the final evaluation result. These errors apply to all methods equally, and therefore the comparison remains fair.

### C. Baselines

Due to the limited public availability of other railway sensor fusion frameworks, we compare our pipeline against two simple baselines:

- *RAW-GNSS*: a first baseline is the directly available unprocessed GNSS measurements. Due to the low update rate of GNSS, this does not provide the same continuity as our framework. Additionally, it provides no knowledge of the current track.
- *Projected-GNSS*: GNSS measurements simply projected onto the closest track.
- *EKF*: the third baseline is a standard EKF, in order to fuse GNSS and odometry measurements, without any prior knowledge of the train tracks. This is implemented using the `robot_pose_ekf` Robot Operating System (ROS) package.
- *Projected-EKF*: the last baseline is a standard EKF, whose estimate is projected onto the closest track in a post-processing step.

### D. Metrics

We report two distinct metrics for each baseline and our method. The first standard metric is the Root Mean Square Error (RMSE) to evaluate the positioning accuracy. For positioning methods that work in non-euclidean coordinates, these are first converted to normal Euclidean coordinates, as to compute the RMSE in the same space for all methods.

The second metric is a track selectivity score. For rail vehicles, it is significantly more important to know on which track the vehicle is located, than where precisely on the

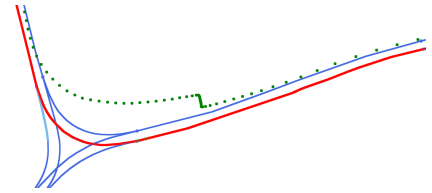


Fig. 6: GNSS signal (green) drifting severely off the track (blue), while the state estimate (red) remains on the correct track.

track it is. We therefore define the track selectivity score as the percentage of time, during which the current position estimate was located on the ground truth track segment. As not all baselines are capable of reporting the current track, this number is only reported for some methods.

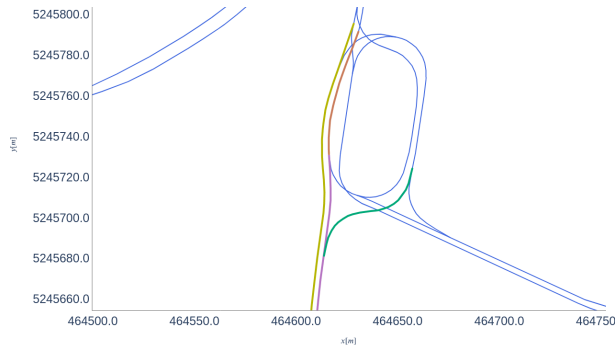
## V. RESULTS

The results for our method and our four baselines are reported in Table I. While GNSS can provide good localization under optimal conditions, and even a good track selectivity, the comparison between different datasets shows the high dependability on good reception. The VIO on its own worked well within the Tram environment, thanks to good lighting and diverse features in urban environments, as well as limited vehicle speeds. It is not expected that VIO generalizes as well to high-speed trains, but there our framework would enable the incorporation of other odometry estimation sensors. Fusing GNSS with VIO in a standard EKF results in a continuous state estimate, but does not improve the overall localization accuracy significantly, as no map data or further global localization is utilized. While integrating the sensor measurements in our path-constrained state estimation pipeline does not result in significant accuracy improvements over raw GNSS, it does significantly improve the track selectivity score. For trains, this is the more relevant positioning metric, as it is vital to know on which track a vehicle is located, while the position along the track is only secondary. This can be seen in Figure 6, where GNSS measurements experience significant disturbances and would even indicate the wrong track, but our fusion pipeline is robust enough to maintain the correct track estimate. The RMSE is only improved by our pipeline in Trajectory 2 and Trajectory 3, where the significant disturbances of the more noisy GNSS are well compensated for using the path-constrained state-estimation.

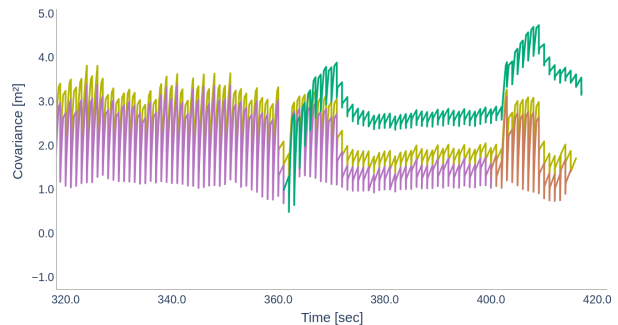
Figure 7 highlights the changes in the covariance of various hypotheses over time. The outlier rejection results in the divergence of some filters, such as ones taking a wrong turn at an intersection, which will then be removed from the collection of active filters. Furthermore, it shows that two hypothesis on parallel tracks will have a similar covariance and covariance propagation, but still with a significant gap to determine the correct track. Bad track selectivity is predominantly observed for short distances directly after complicated intersections, where neither of the noisy sensors is providing a consistent motion estimate.

TABLE I: Positioning accuracy reported in terms of RMSE and Track Selectivity for all methods on 3 different trajectories.

	Trajectory 1		Trajectory 2		Trajectory 3	
	RMSE	Track Selectivity	RMSE	Track Selectivity	RMSE	Track Selectivity
Raw-GNSS	4.10 m	n/a	18.52 m	n/a	43.71 m	n/a
Projected-GNSS	<b>2.31 m</b>	92 %	17.73 m	59.7 %	41.83 m	49.8 %
EKF	10.63 m	n/a	22.20 m	n/a	43.07 m	n/a
Projected-EKF	6.27 m	90.6 %	20.79 m	69.7 %	41.31 m	50.04 %
Ours	4.78 m	<b>94.9 %</b>	<b>18.09 m</b>	<b>85.2 %</b>	<b>22.63 m</b>	<b>81.4 %</b>



(a) Positions of various filters (yellow, brown, violet and green) on different tracks (blue).



(b) Positioning covariance of various filters over time

Fig. 7: The position of various filters can be seen on the left and their respective covariances on the right. A difference in covariance between parallel tracks is observable, as well as an increasing covariance for

## VI. CONCLUSION

In this paper, we introduced a path-constrained state estimation framework for fusing arbitrary sensor modalities together with public map data to robustly and accurately localize rail vehicles. For this, we developed a novel multi-hypothesis EKF, utilizing a curve coordinate formulation to predict the vehicle’s motion along known train tracks and fuse sensor measurements into the current state.

We demonstrate the accuracy and reliability of our pipeline using three different datasets recorded on local trams. Many intersections and limited GNSS availability make this a challenging testing ground. Our experiments show that our pipeline significantly improves localization accuracy and robustness over common existing solutions.

We plan to expand this work together with our event-based railway mapping framework [55] into a full on-board high-speed railway Simultaneous Localization and Mapping (SLAM) framework. Event-based vision could provide both the required odometry estimation, as well as global localization through the detection and mapping of infrastructure elements.

## REFERENCES

- [1] P. Stanley, *ETCS for Engineers*, 1st ed. TZ - Verl. & Print GmbH, 2011.
- [2] J. Beugin and J. Marais, “Simulation-Based Evaluation of Dependability and Safety Properties of Satellite Technologies for Railway Localization,” *Transportation Research Part C: Emerging Technologies*, vol. 22, pp. 42–57, 2012.
- [3] J. Marais, J. Beugin, and M. Berbineau, “A Survey of GNSS-Based Research and Developments for the European Railway Signaling,” *IEEE Transactions on Intelligent Transportation Systems*, vol. 18, no. 10, pp. 2602–2618, 2017.
- [4] T. Albrecht, K. Luddecke, and J. Zimmermann, “A Precise and Reliable Train Positioning System and Its Use for Automation of Train Operation,” in *IEEE International Conference on Intelligent Rail Transportation Proceedings (ICIRT)*, 2013, pp. 134–139.
- [5] C. Amatetti, T. Polonelli, E. Masina, C. Moatti, D. Mikhaylov, D. Amato, A. Vaneli-Coralli, M. Magno, and L. Benini, “Towards the Future Generation of Railway Localization and Signaling Exploiting Sub-Meter RTK GNSS,” in *IEEE Sensors Applications Symposium (SAS)*, 2022, pp. 1–6.
- [6] J. Liu, J.-c. Li, B.-g. Cai, and J. Wang, “Test and Evaluation of GNSS-based Railway Train Positioning under Jamming Conditions,” in *IEEE International Conference on Systems, Man, and Cybernetics (SMC)*, 2020, pp. 1459–1464.
- [7] J. Otegui, A. Bahillo, I. Lopetegi, and L. E. Diez, “A Survey of Train Positioning Solutions,” *IEEE Sensors Journal*, vol. 17, no. 20, pp. 6788–6797, 2017.
- [8] M. Sengupta, “Choice of sensor fusion framework for train positioning system,” *Computers in Railways XVII: Railway Engineering Design and Operation*, vol. 199, pp. 53–64, 2020.
- [9] F. Caron, M. Davy, E. Duflos, and P. Vanheegehe, “Particle Filtering for Multisensor Data Fusion With Switching Observation Models: Application to Land Vehicle Positioning,” *IEEE Transactions on Signal Processing*, vol. 55, no. 6, pp. 2703–2719, 2007.
- [10] F. Gustafsson, “Particle Filter Theory and Practice with Positioning Applications,” *IEEE Aerospace and Electronic Systems Magazine*, vol. 25, no. 7, pp. 53–82, 2010.
- [11] S. J. Julier and J. K. Uhlmann, “Unscented Filtering and Nonlinear Estimation,” *Proceedings of the IEEE*, vol. 92, no. 3, pp. 401–422, 2004.
- [12] S. Chen, “Kalman Filter for Robot Vision: A Survey,” *IEEE Transactions on Industrial Electronics*, vol. 59, no. 11, pp. 4409–4420, 2011.
- [13] M. Bloesch, M. Burri, H. Sommer, R. Siegwart, and M. Hutter, “The Two-State Implicit Filter Recursive Estimation for Mobile Robots,” *IEEE Robotics and Automation Letters (RA-L)*, vol. 3, no. 1, pp. 573–580, 2017.
- [14] S. Leutenegger, S. Lynen, M. Bosse, R. Siegwart, and P. Furgale, “Keyframe-Based Visual-Inertial SLAM Using Nonlinear Optimization,” *The International Journal of Robotics Research (IJRR)*, vol. 34, no. 3, pp. 314–334, 2015.
- [15] R. Mascaro, L. Teixeira, T. Hinzmann, R. Siegwart, and M. Chli, “GOMSF: Graph-Optimization Based Multi-Sensor Fusion for robust

- UAV Pose estimation,” in *2018 IEEE International Conference on Robotics and Automation (ICRA)*. IEEE, 2018, pp. 1421–1428.
- [16] X. Weng, B. Ivanovic, and M. Pavone, “MTP: Multi-hypothesis Tracking and Prediction for Reduced Error Propagation,” in *Proceedings of the IEEE Intelligent Vehicles Symposium (IV)*, 2022, pp. 1218–1225.
- [17] L. Bernreiter, A. Gawel, H. Sommer, J. Nieto, R. Siegwart, and C. C. Lerma, “Multiple Hypothesis Semantic Mapping for Robust Data Association,” *IEEE Robotics and Automation Letters (RA-L)*, vol. 4, no. 4, pp. 3255–3262, 2019.
- [18] K. Tan, Q. Ji, L. Feng, and M. Törngren, “Shape Estimation of a 3D Printed Soft Sensor Using Multi-Hypothesis Extended Kalman Filter,” *IEEE Robotics and Automation Letters (RA-L)*, vol. 7, no. 3, pp. 8383–8390, 2022.
- [19] T. Heidenreich, J. Spehr, and C. Stiller, “LaneSLAM – Simultaneous Pose and Lane Estimation Using Maps with Lane-Level Accuracy,” in *IEEE International Conference on Intelligent Transportation Systems (ITSC)*, 2015, pp. 2512–2517.
- [20] D. Petrich, T. Dang, G. Breuel, and C. Stiller, “Assessing Map-Based Maneuver Hypotheses Using Probabilistic Methods and Evidence Theory,” in *IEEE International Conference on Intelligent Transportation Systems (ITSC)*, 2014, pp. 995–1002.
- [21] K. Krishanth, R. Tharmarasa, T. Kirubarajan, P. Valin, and E. Meger, “Prediction and Retrodiction Algorithms for Path-Constrained Targets,” *IEEE Transactions on Aerospace and Electronic Systems*, 2014.
- [22] S. Wijesoma, K. W. Lee, and J. I. Guzman, “On the Observability of Path Constrained Vehicle Localisation,” in *IEEE International Conference on Intelligent Transportation Systems (ITSC)*, 2006, pp. 1513–1518.
- [23] M. A. Quddus, W. Y. Ochieng, and R. B. Noland, “Current Map-Matching Algorithms for Transport Applications: State-of-the Art and Future Research Directions,” *Transportation Research Part C: Emerging Technologies*, vol. 15, no. 5, pp. 312–328, 2007.
- [24] D. Bernstein and A. Kornhauser, “An Introduction to Map Matching for Personal Navigation Assistants,” US Transportation Collection.
- [25] K. W. Lee, S. Wijesoma, and J. I. Guzmán, “A Constrained SLAM Approach to Robust and Accurate Localisation of Autonomous Ground Vehicles,” *Robotics and Autonomous Systems*, vol. 55, no. 7, pp. 527–540, 2007.
- [26] J. Liu, B.-g. Cai, and J. Wang, “A GNSS/Trackmap Cooperative Train Positioning Method for Satellite-Based Train Control,” in *IEEE International Conference on Intelligent Transportation Systems (ITSC)*, 2014, pp. 2718–2724.
- [27] W. Jiang, Y. Liu, B. Cai, C. Rizos, J. Wang, and Y. Jiang, “A New Train Integrity Resolution Method Based on Online Carrier Phase Relative Positioning,” *IEEE Transactions on Vehicular Technology*, vol. 69, no. 10, pp. 10 519–10 530, 2020.
- [28] Z. Cao, J. Liu, W. Jiang, B. Cai, and J. Wang, “INS/Odometer/Trackmap-aided Railway Train Localization under GNSS Jamming Conditions,” in *Proceedings of the IEEE Intelligent Vehicles Symposium (IV)*, 2022, pp. 427–434.
- [29] H.-J. Chu, G.-J. Tsai, K.-W. Chiang, and T.-T. Duong, “GPS/MEMS INS Data Fusion and Map Matching in Urban Areas,” *Sensors*, vol. 13, no. 9, pp. 11 280–11 288, 2013.
- [30] M. Cossaboom, J. Georgy, T. Karamat, and A. Noureldin, “Augmented Kalman Filter and Map Matching for 3D RISS/GPS Integration for Land Vehicles,” *International Journal of Navigation and Observation*, vol. 2012, pp. 1–16, 2012.
- [31] S. Brakatsoulas, D. Pfoser, R. Salas, and C. Wenk, “On Map-Matching Vehicle Tracking Data,” in *Proceedings of the International Conference on Very Large Data Bases*, 2005, pp. 853–864.
- [32] J. Yuan, Y. Zheng, C. Zhang, X. Xie, and G.-Z. Sun, “An Interactive-Voting Based Map Matching Algorithm,” in *International Conference on Mobile Data Management*, 2010, pp. 43–52.
- [33] Y. Lou, C. Zhang, Y. Zheng, X. Xie, W. Wang, and Y. Huang, “Map-Matching for Low-Sampling-Rate GPS Trajectories,” in *Proceedings of the International Conference on Advances in Geographic Information Systems*, 2009, p. 352.
- [34] C. Peng and D. Weikersdorfer, “Map as The Hidden Sensor: Fast Odometry-Based Global Localization,” in *IEEE International Conference on Robotics and Automation (ICRA)*, 2020, pp. 2317–2323.
- [35] T. Kirubarajan, Y. Bar-Shalom, K. Pattipati, I. Kadar, B. Abrams, and E. Eadan, “Tracking Ground Targets with Road Constraints Using an IMM Estimator,” in *IEEE Aerospace Conference Proceedings*, vol. 5, 1998, pp. 5–12.
- [36] O. Heirich, “Bayesian Train Localization with Particle Filter, Loosely Coupled GNSS, IMU, and a Track Map,” *Journal of Sensors*, vol. 2016, pp. 1–15, 2016.
- [37] M. Lauer and D. Stein, “A Train Localization Algorithm for Train Protection Systems of the Future,” *IEEE Transactions on Intelligent Transportation Systems*, vol. 16, no. 2, pp. 970–979, 2014.
- [38] C. Hasberg, S. Hensel, and C. Stiller, “Simultaneous Localization and Mapping for Path-Constrained Motion,” *IEEE Transactions on Intelligent Transportation Systems*, vol. 13, no. 2, pp. 541–552, 2012.
- [39] C. Williams, “The Next ETCS Level?” in *IEEE International Conference on Intelligent Rail Transportation Proceedings (ICIRT)*, 2016, pp. 75–79.
- [40] A. M. Kostrominov, O. N. Tyulyandin, A. B. Nikitin, M. N. Vasilenko, and A. T. Osminin, “RFID-Based Navigation of Subway Trains,” in *IEEE East-West Design & Test Symposium*, 2020, pp. 1–6.
- [41] W. Zheng, S. Ma, Z. Hua, H. Jia, and Z. Zhao, “Train Integrated Positioning Method Based on GPS/INS/RFID,” in *Chinese Control Conference (CCC)*, 2016, pp. 5858–5862.
- [42] S. Hensel and C. Hasberg, “Probabilistic Landmark Based Localization of Rail Vehicles in Topological Maps,” in *IEEE/RSJ International Conference on Intelligent Robots and Systems (IROS)*, 2010, pp. 4824–4829.
- [43] O. Heirich, B. Siebler, and E. Hedberg, “Study of Train-Side Passive Magnetic Measurements with Applications to Train Localization,” *Journal of Sensors*, vol. 2017, pp. 1–10, 2017.
- [44] O. Heirich, A. Steingass, A. Lehner, and T. Strang, “Velocity and Location Information from Onboard Vibration Measurements of Rail Vehicles,” in *Proceedings of the International Conference on Information Fusion*, 2013, pp. 1835–1840.
- [45] J. Wohlfeil, “Vision Based Rail Track and Switch Recognition for Self-Localization of Trains in a Rail Network,” in *Proceedings of the IEEE Intelligent Vehicles Symposium (IV)*, 2011, pp. 1025–1030.
- [46] W. Nai, Y. Chen, X. Zhang, X. Lei, and D. Dong, “A Train Positioning Algorithm Based on Inflexion Analysis by Using Sets of Distance Measurement Data Collected from On-Board Laser Ranging Equipments,” in *IEEE International Conference on Computer and Communications (ICCC)*, 2017, pp. 901–904.
- [47] T. Daooust, F. Pomerleau, and T. D. Barfoot, “Light at the End of the Tunnel: High-Speed LiDAR-Based Train Localization in Challenging Underground Environments,” in *Conference on Computer and Robot Vision (CRV)*, 2016, pp. 93–100.
- [48] B. Allotta, P. D’Adamio, M. Malvezzi, L. Pugi, A. Ridolfi, and G. Vettori, “A Localization Algorithm for Railway Vehicles,” in *IEEE International Instrumentation and Measurement Technology Conference (I2MTC)*, 2015, pp. 681–686.
- [49] F. Tschopp, T. Schneider, A. W. Palmer, N. Nourani-Vatani, C. Cadena, R. Siegwart, and J. Nieto, “Experimental Comparison of Visual-Aided Odometry Methods for Rail Vehicles,” *IEEE Robotics and Automation Letters (RA-L)*, vol. 4, no. 2, pp. 1815–1822, 2019.
- [50] F. Tschopp, “Visual Positioning for Railway Vehicles,” Ph.D. dissertation, ETH Zurich, 2021.
- [51] H. Winter, S. Luthardt, V. Willert, and J. Adamy, “Generating Compact Geometric Track-Maps for Train Positioning Applications,” in *Proceedings of the IEEE Intelligent Vehicles Symposium (IV)*, 2019, pp. 1027–1032.
- [52] Z. Berman, “Outliers rejection in kalman filtering — some new observations,” in *2014 IEEE/ION Position, Location and Navigation Symposium - PLANS 2014*, 2014, pp. 1008–1013.
- [53] J. Nikolic, J. Rehder, M. Burri, P. Gohl, S. Leutenegger, P. T. Furgale, and R. Siegwart, “A synchronized visual-inertial sensor system with fpga pre-processing for accurate real-time slam,” in *2014 IEEE International Conference on Robotics and Automation (ICRA)*, 2014, pp. 431–437.
- [54] P. Furgale, J. Rehder, and R. Siegwart, “Unified Temporal and Spatial Calibration for Multi-Sensor Systems,” in *IEEE/RSJ International Conference on Intelligent Robots and Systems (IROS)*, 2013, pp. 1280–1286.
- [55] F. Tschopp, C. von Einem, A. Cramariuc, D. Hug, A. W. Palmer, R. Siegwart, M. Chli, and J. Nieto, “Hough<sup>2</sup>Map – Iterative Event-Based Hough Transform for High-Speed Railway Mapping,” *IEEE Robotics and Automation Letters (RA-L)*, vol. 6, no. 2, pp. 2745–2752, 2021.